Radiation Degradation Mechanisms in Laser Diodes

A. H. Johnston, *Fellow, IEEE,* and T. F. Miyahira
Jet Propulsion Laboratory
Pasadena, California

Abstract *– Degradation mechanisms are investigated for laser diodes fabricated with different materials and wavelengths between 660 and 1550 nm. A new approach is developed that evaluates degradation below the laser threshold to determine the radiation-induced recombination density. This allows mechanisms at high injection, such as Auger recombination, to be separated from low-injection damage. New results show that AlGaInP lasers in the visible region are nearly an order of magnitude more resistant to radiation than devices fabricated with AlGaAs or AlGaAsP at longer wavelengths.*

I. Introduction

Modern laser diodes are complex devices that take advantage of special material properties, narrow regions for quantum carrier confinement, and the ability to grow many different layers within a single structure with precisely controlled thickness and composition to form highly efficient lasers[1,2]. Only a limited number of studies have been made of radiation degradation of advanced laser diodes, and their interpretation is made more difficult by the continuing evolution of laser diode technology [3-7]. The push towards better lasers has stressed decreasing threshold current, improving linearity, and extending lasers to different wavelength ranges, including the difficult region between 900 and 1100 nm where it is not possible to obtain close lattice matching in material properties.

This paper discusses radiation degradation mechanisms for in-plane laser diodes with wavelengths between 650 and 1550 nm, including new ways of examining laser degradation that provide methods to investigate damage mechanisms, and recommendations for test methods that improve the ability to compare results from different laboratories. Although improved understanding of the underlying mechanisms may not be necessary for applications of lasers at low radiation levels, it is essential in order to interpret laser degradation at high levels, such as the recent work by Kalavagunta, *et al.* for GaAs VCSELs [7].

The research in this paper was carried out at the Jet Propulsion Laboratory, California Institute of Technology, under contract with the National Aeronautics and Space Administration (NASA).

II. Semiconductor Laser Operation

Semiconductor lasers can be fabricated with a variety of structures including ridge lasers where the active region is formed on an isolated mesa at the top; buried crescent lasers where the active region is laterally isolated by separate heterostructures or deposited oxide regions; and double channel buried heterostructures. All of these geometries are variations on the stripe laser concept, where current injection is restricted to a narrow stripe region within the structure.

In addition to these basic geometrical designs, two basic methods have emerged to reduce threshold current. The first is the use of very thin layers that confine carriers by quantum confinement; and the second is fabrication of deliberately strained materials that are thin enough to avoid lattice mismatch effects. Strained lattices are essential for InGaAs (~ 980 nm), and are also useful to improve the characteristics of InGaAsP lasers in the 1300-1550 nm region.

Modern in-plane lasers are complex structures, as illustrated in the multiple quantum layer InGaAsP laser of Fig. 1. The active region is a thin undoped region with four quantum wells. Cladding layers above and below the active region form heterostructures for carrier confinement. Additional layers are used for optical confinement. The typical width of the active region is 2 μm, with a cavity length of 250-700 μm.

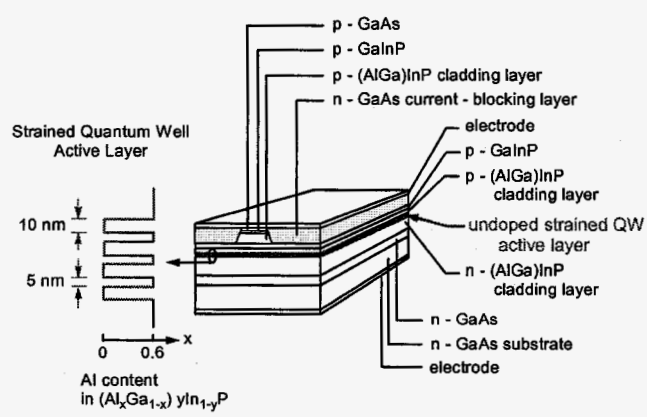

Fig. 1. Diagram of a modern multiple-quantum well in-plane laser diode.

Several different material systems are used in laser fabrication. Some important properties are listed in Table 2.

Table 2
Material Systems for Lasers Discussed in this Work

Material	Wavelength Range (μm)	Key Technical Issues
AlGaInP	600-700	Developed for high-intensity applications
AlGaAs	630-950	Used for heterostructure lasers beginning in 1970
InGaAs	900-1100	Requires strained layers because of lattice mismatch
InGaAsP	1100-1550	Material has high Auger recombination rate

III. Experimental Procedure

A. Devices Selected for Study

Several different types of lasers were used in the study. Some of the key properties are listed below. The first two lasers use AlGaInP. They have much higher power output compared to the other three types of lasers.

Table 3
Lasers Used for Experimental Work in This Study

Device	Manufact.	λ (μm)	I_{th} (mA)	P_{out} (mW)	Material
HL6501	Hitachi	660	45	35	AlGaInP
ML101J8	Mitsubishi	660	57	45	AlGaInP
L9805	Roitman	980	15	50	InGaAs
ML725	Mitsubishi	1310	5	10	InGaAsP
C1550	Lasermate	1550	10	6	InGaAsP

In addition to new results for these lasers, we will also use results from previous laser studies[5]. The experimental method used in the earlier work was essentially identical, except that all measurements were made at a single temperature (25 °C).

B. Irradiation and Measurement Procedure

Devices were irradiated with 51-MeV protons at the University of California, Davis, cyclotron. They were irradiated without bias (all pins shorted) in a series of irradiation steps, removing the devices after each radiation level for characterization measurements.

Measurements were made by placing the lasers in a test fixture that controlled the case temperature to a set value, with a precision of ± 0.2 °C. The measurements that were made included the optical power within a narrow acceptance angle using an external photodiode, and the forward voltage. A silicon photodetector was used for lasers with wavelength shorter than 1000 μm. An InGaAs photodetector was used for lasers with longer wavelength. An Agilent semiconductor parameter analyzer was used to make the measurements. For the series of experiments reported in this work easurements were made at three different temperatures: 20, 30 and 40 °C to determine how the temperature coefficient of basic laser properties was affected by radiation damage.

IV. Test Results

A. Power Output Characteristics

The most critical parameter for laser diodes is threshold current. Fig. 2 shows the effect of proton damage on the optical power of the Lasermate 1550 nm laser diode as the forward current increases from very low currents to the region where laser operation begins. The optical power increases abruptly after the forward current reaches the threshold current, which is determined by fitting a straight line to the optical power curve above threshold. The slope efficiency is nearly constant above threshold, although it decreases slightly after irradiation.

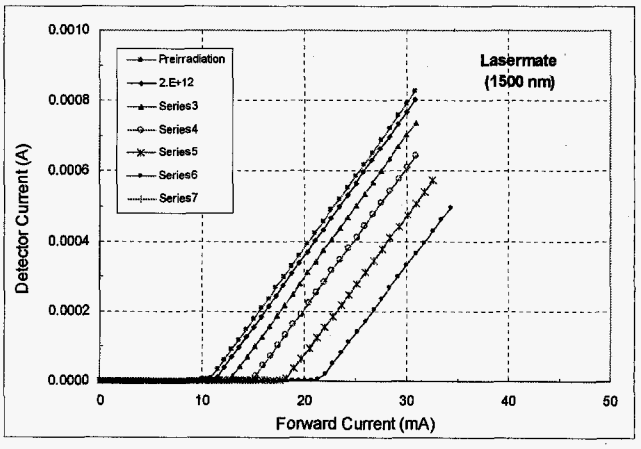

Fig. 2. Optical power characteristics for the Lasermate 1550 nm laser diode after several irradiations.

The threshold current after the highest radiation level has nearly doubled. The increase in threshold current is accompanied by an increase in forward voltage (at threshold) from approximately 0.9 to 1 V, a change that is large enough to alter current flow within the structure because of the large increase in non-radiative recombination current. Thus, a great deal more damage has actually taken place in the device that is not evident from the relatively small increase in threshold current.

The results in Fig. 2 are typical of those exhibited by the other types of lasers in the study. In all cases there was a relatively abrupt transition from the LED mode below threshold to the high optical power region that is typical of laser operation, although that transition was less abrupt for the two AlGaInP lasers (660 nm). To first order, the fractional change in threshold current increases linearly with fluence, as shown in Fig. 3 (there are slight deviations from linearity that will be discussed in the next section). The two AlGaInP lasers exhibited smaller changes after radiation compared to the other laser types. The apparent nonlinearity at low fluences for those two devices is affected by the ●1% accuracy of the measurements.

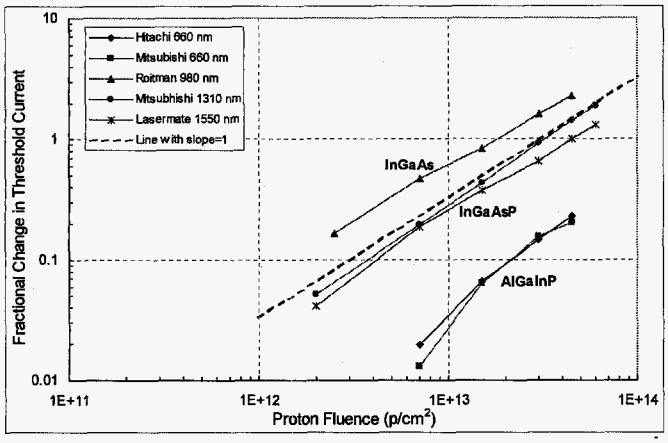

Fig.3. Fractional change in threshold current for the five types of laser diodes, measured at 20 °C.

Slope efficiency was slightly affected by radiation damage. Fig. 4 shows the percent change in slope efficiency for the two AlGaAsP laser types vs. proton fluence.

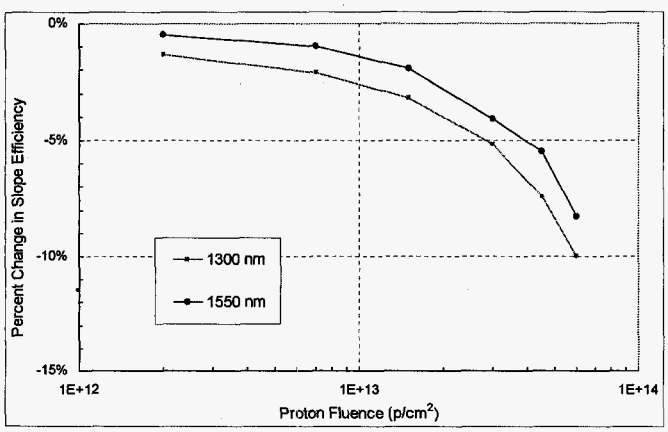

Fig.4. Percent change in slope efficiency for the two types of AlGaAsP laser diodes.

B. Temperature Sensitivity

The main purpose of measuring devices at different temperatures was to provide diagnostic information for Auger recombination, which is the reason for the larger temperature sensitivity of 1300 and 1550 nm lasers fabricated with AlGaAsP (the temperature dependence of the other threee laser types is much lower, and was essentially unaffected by radiation). The temperature dependence of the AlGaAsP lasers decreased after irradiation, as shown in Fig. 5. The 1550 nm laser was more strongly affected by temperature prior to irradiation, which is consistent with results in the literature [8].

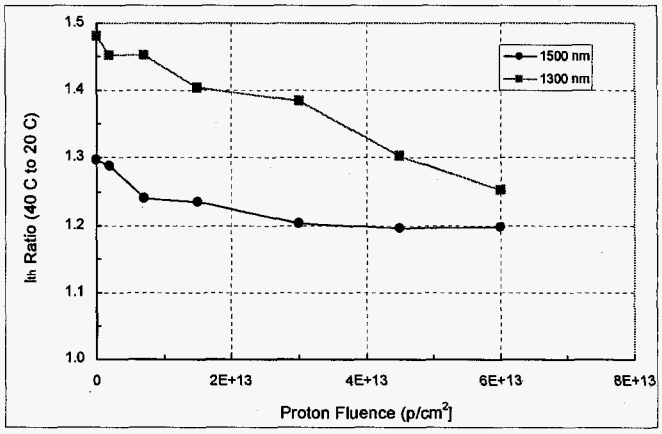

Fig. 5. Change in temperature sensitivity of threshold current after irradiation for the two types of laser diodes using AlGaAsP.

V. Discussion

A. Low Injection Degradation

Degradation in these lasers is much greater at low injection conditions, when the laser operates in the LED mode. Fig. 6 shows the results of Fig.2, plotted logarithmically to reveal details at low currents. The light output (due to radiative recombination) is reduced far more at currents below the threshold current compared to the changes that occur in threshold current when the device enters the laser mode, and light output is dominated by stimulated emission. This suggests that evaluation of device behavior at low injection may be a more fundamental way to evaluate damage in the structure and the material than threshold current.

Degradation of the 1550 nm in the LED mode can be evaluated using the Rose-Barnes equation [9], where the ratio of the initial light output to the light output after irradiation is described by the power law

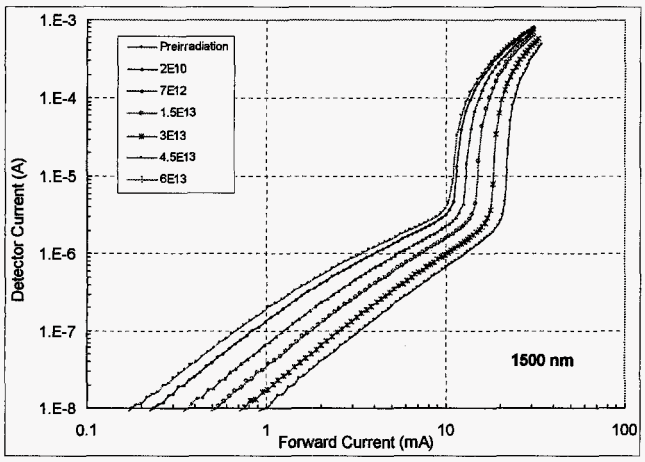

Fig. 6. Logarithmic plot of optical power of the Lasermate 1550 nm laser diode shown previously in Fig. 2.

$$\left[\frac{Io}{I}\right]^n - 1 = Ko\tau\Phi \qquad (1)$$

where I_o is the initial light output, I is the light output after irradiation, n is an exponent between 2/3 and 1, K_o is a damage constant, τ is the minority carrier lifetime, and Φ is the particle fluence. Fig. 7 shows how degradation at a forward current of 9.5 mA, approximately 15% below the pre-irradiation threshold current, is described by Eq. 1 with n = 1. The data fit a straight line remarkably well up to a fluence of 3 x 10^{13} p/cm^2, but departs from linearity at higher fluences. This indicates that an additional loss mechanism begins to contribute at high fluences, even under low injection conditions below the laser threshold.

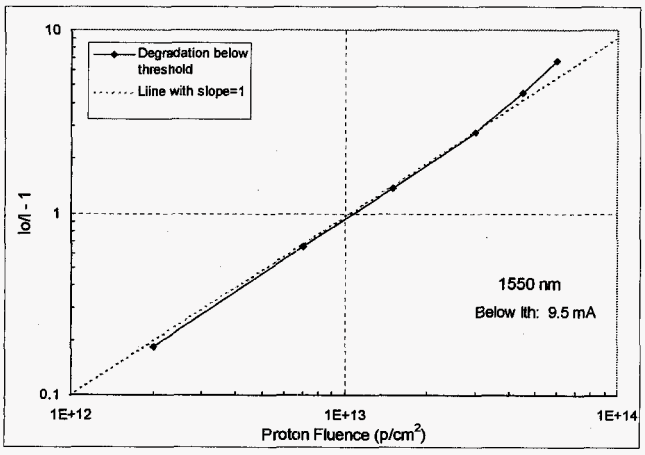

Fig. 7. Evaluation of degradation of light output below the laser threshold using the Rose-Barnes equation (n = 1) for the Lasermate 1550 nm laser diode.

There is a corresponding departure from linearity when laser threshold current is plotted vs. fluence, as shown in Fig. 8. However, the data in Fig. 8 are not taken at a fixed current, but at successively higher current densities as the threshold current increases after degradation.

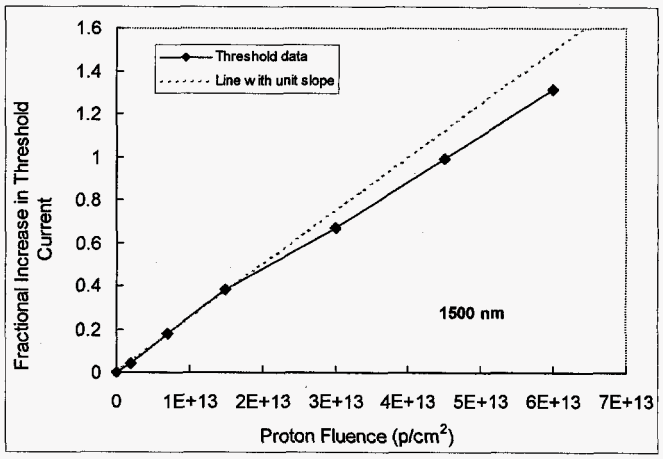

B. Derivative Plots

Another way to analyze radiation degradation is to plot the derivative of the optical power (with respect to forward current) as a function of forward current. Fig. 9 shows an example for a 1300 nm laser (Fermionics) from our earlier study [5]. The optical power derivative rises abruptly above threshold, decreasing slowly at higher currents because of internal losses. The key point in this figure is that the value of the derivative after irradiation is essentially superimposed on the operating conditions of the laser prior to irradiation.

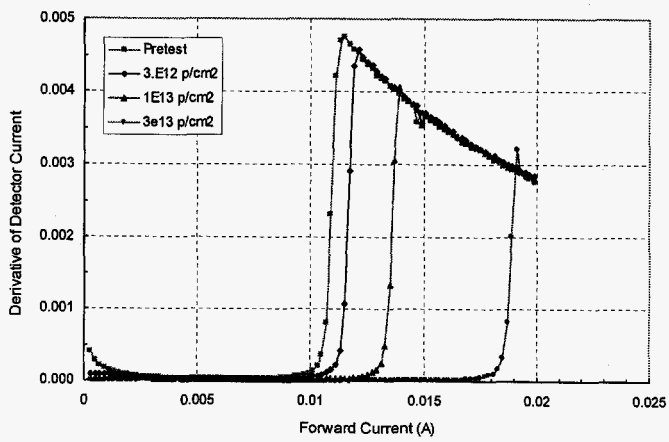

Fig. 9. Derivative of optical power vs. forward current for a Fermionics laser diode (wavelength 1300 nm). Values after irradiation are essentially superimposed on the pre-irradiation characteristics.

A similar plot is shown in Fig. 10 for the Lasermate 1550 nm laser diode that was irradiated in the present study. In this case the derivative remains nearly constant with current before irradiation. After irradiation the value of the derivative is about 10% lower, implying that an additional loss mechanism is taking place in this device that does not occur in the 1300 nm laser shown in the previous figure. One potential mechanism is Auger recombination.

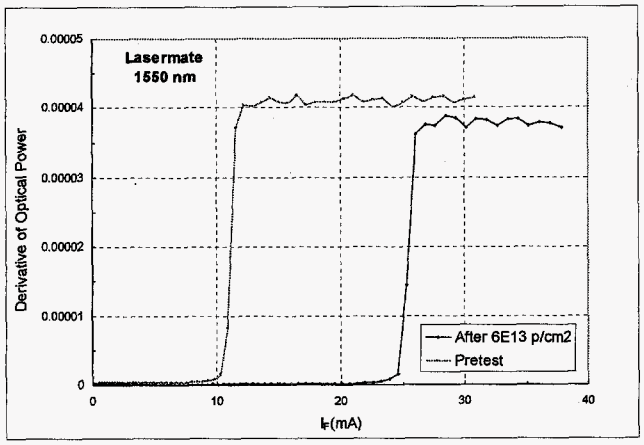

Fig. 10. Derivative of optical power vs. forward current for the 1550 nm Lasermate laser diode.

C. Damage Mechanisms

Recombination Processes and Threshold Conditions

Band-to-band recombination accompanied by photon emission is the dominant recombination mechanism for high-quality direct bandgap materials except at very low injection levels. Nearly all treatments of laser threshold conditions assume that non-radiative (N.R.) recombination is negligible near the threshold region, but that assumption is clearly incorrect for lasers after irradiation because the primary effect of displacement damage is the introduction of traps that increase N.R. recombination.

Threshold conditions for a semiconductor laser depend on increasing the radiative recombination rate to the point where photons from radiative recombination that are aligned with the preferred direction in the laser cavity reach the intensity level for stimulated emission to become the dominant recombination process. Photons produced by radiative recombination are produced in random directions, and consequently only a small fraction of the total number of photons are actually involved in the stimulated emission process.

Gain in a laser structure depends on material properties as well as the physical structure of the laser. The overall conditions for operation of an in-plane laser can be described for the laser *cavity* by [10,11]

$$\Gamma G_{th} = \alpha_i + \alpha_m = \frac{1}{v_g \tau_p} \qquad (2)$$

where Γ is the mode confinement factor, G_{th} is the threshold gain condition, α_i is the internal optical loss within the cavity, α_m is the effective loss in the two mirrors (that term also contains a length factor which is unimportant for our discussion), v_g is the group velocity and τ_p is the photon decay rate in the laser cavity.

There are several recombination effects that depend on carrier density. Just below threshold the recombination rate is given by

$$R = An + Bn^2 + Cn^3 = \frac{n_{th}}{\tau} \qquad (3)$$

where A is the bulk recombination rate, B is the spontaneous band-to-band recombination rate, C is the Auger recombination rate, n is the carrier concentration, n_{th} is the carrier concentration at threshold, and τ is the effective lifetime.

The coefficient B has nearly the same value – approximately 10^{-10} cm^3/s - for AlGaAs, InGaAs and InGaAsP. As a result, carrier densities above of 10^{18} cm^{-3} are required to increase the spontaneous recombination rate to the point where the photon density is sufficiently high to reach threshold. When the bulk recombination rate increases due to radiation damage, the carrier concentration must increase to overcome the loss term that is linear with n, increasing the carrier density required at threshold. For materials with high Auger recombination, there is effectively a race between the n^2 dependence of spontaneous recombination and the n^3 dependence for Auger losses.

We can examine the relative effect of these terms by plotting the square root of optical power vs. current, following an approach used by Minch, *et al.* [12] Those results are shown in Fig. 11. Prior to irradiation, the boundaries between low injection where N.R recombination is the dominant process and intermediate injection where radiative

recombination dominates can clearly be delineated by the change in slope, from 1 at low injection to 2 when radiative recombination dominates.

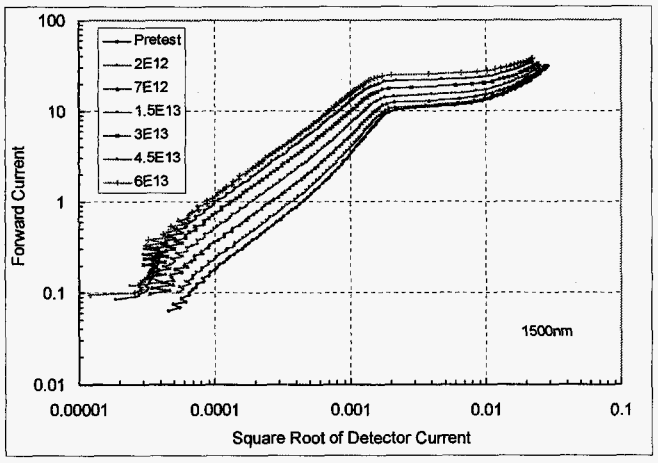

Fig. 11. Plot of the square root of optical power vs. forward current. The transition from a slope of one to a slope of two occurs when radiative recombination becomes the dominant loss process.

After the first three irradiations the change in slope is clearly evident, but at high radiation levels N.R. recombination dominates the process making it impossible to determine the point where radiation recombination overcomes bulk recombination loss (this clearly occurs, because it is a fundamental requirement for laser operation). This figure illustrates how dominant the N.R. recombination becomes after irradiation.

D. Threshold Current Dependence on Fluence

For many lasers, the threshold current increases linearly with current. There are others – including the 1300 nm laser used as an example in this paper – where the dependence of threshold current on fluence is slightly sublinear. This is illustrated in Fig. 12, along with earlier results for a 980 nm strained quantum well laser from Evans, et al. [3]. The 5.5-MeV protons used in the earlier work have been adjusted to equivalent 50-MeV protons in this figure, using NIEL results for GaAs.

The conditions for laser operation are directly affected by material gain. Material gain for GaAs and InGaAs are shown in Fig. 13 [11] to illustrate the dependence of gain on carrier density. There is a relatively broad minimum in this relationship. When radiation damage increases threshold current, it moves the operating point to the right. Losses resulting from radiation damage are compensated by increasing the current density to produce higher material gain. The gain curves are nonlinear for large changes in operating conditions, but linearity is often assumed for small changes. The relative effect of an increase in carrier density to compensate for radiation damage depends not only on the amount of damage, but also on the differential material gain, which varies considerably for different material types. Material gain is also affected by basic laser design, such as quantum well structures. Because of these factors we expect departures from linearity that can be either sublinear or superlinear.

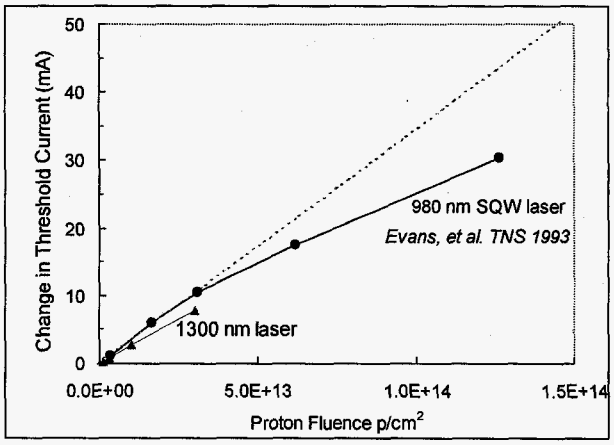

Fig. 12. Nonlinear dependence of threshold current change at higher fluences for two different types of lasers.

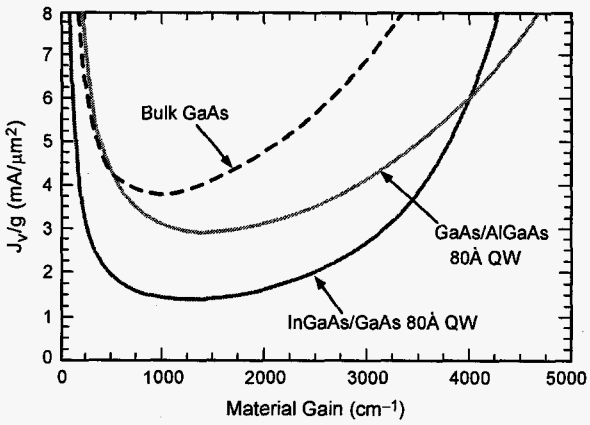

Fig. 13. Bulk recombination current/gain vs. material gain for GaAs and InGaAs.

Threshold current is only one factor in degraded lasers. If a degraded laser is used with the higher current required to produce equivalent amounts of optical power the carrier density will be much higher, introducing other loss mechanisms that will cause the slope efficiency to decrease. Because of the high carrier density required for laser operation, doping levels are typically > 5 x 10^{17} cm^{-3} for the various layers used in laser diodes. Consequently, carrier removal [14,15] is not expected to be important for

fluences below approximately 10^{14} p/cm^2, but will likely be important at higher fluences. (Carrier removal rates are on the order of 10 cm^{-1} for 50-MeV protons).

E. Temperature Dependence

Threshold current depends on temperature.

Laser threshold current increases with temperature. The dependence is usually described with the exponential relationship

$$I_{th} = I_o \exp\left(\frac{T}{T_o}\right) \qquad (4)$$

where I_{th} is the threshold current at temperature T in Kelvin, I_o is a current defined as the characteristic current, and T_o is the characteristic temperature. Eq. 4 was proposed by Pankove [16], and is widely used even though it is oversimplified and only describes temperature dependence over a limited range.

The temperature dependence depends on optical gain, which is inherently temperature dependent because of broadening of the electron and hole distributions [8,16]. It also depends on recombination processes. T_o is larger for AlGaAs compared to InGaAsP and AlGaAsP because Auger recombination is lower in AlGaAs. Typical values for T_o at 300 K are 150-200 for InGaAs and 50-70 for the other materials. However, actual values of T_o are about 100 K for the 1550 nm devices in our study.

The threshold current of the 1310 and 1550 nm lasers that was measured prior to irradiation was more sensitive to temperature than the threshold current of the other three types of lasers. T_o was approximately 98 K for the 1550 nm devices and 150 K for the 1310 nm lasers. Those values are higher (implying lower temperature dependence, as shown in Eq. 1) than for older values in the literature, but the older values do not take into account the effects of quantum-well confinement, which reduce temperature sensitivity [17].

The relative contribution of Auger recombination for InGaAsP at threshold has been estimated at 50% for a wavelength of 1.3 μm, and 80-90% at 1.5 μm [18]. Those values apply to optimized devices at room temperature. Auger recombination is negligible for AlGaAs. From Eq. 3, Auger recombination depends on N^3, and therefore we expect more degradation at higher temperature for materials where Auger recombination makes a significant contribution to overall loss. The cubic dependence will introduce a nonlinearity in threshold current change with fluence at sufficiently high levels, as well as changing the slope efficiency.

Other mechanisms can be important for different types of lasers, including leakage through heterostructures in the InGaAsP system, which has lower barrier heights compared to AlGaAs. Leakage current depends exponentially on barrier height divided by kT, where k is the Boltzmann constatnt and T is temperature in Kelvin.

VI. Conclusions

This paper has discussed mechanisms and characterization methods for displacement damage in laser diodes. InGaAsP laser diodes were used as examples, because that material has a much higher Auger recombination coefficient compared to laser diodes with wavelengths below 1300 nm that use other III-V materials. A superlinear dependence of threshold voltage on fluence was observed for the 1550 nm laser diode, but not for lasers that operate at a nominal wavelength of 1300 nm. That result is consistent with the higher Auger recombination coefficient at 1550 nm.

Measurements at injection levels below the laser threshold current can be used to distinguish the transition point between non-radiative losses and radiative recombination in lasers with moderate levels of damage. However, at high radiation levels non-radiative losses dominate, and the dependence of threshold current on fluence becomes sublinear except for the 1550 nm lasers.

Laser diodes in the visible region that are fabricated with AlGaInP have a lower damage constant compared to the other lasers in the study. The improved hardness is likely due to the importance of tunneling mechanisms in charge transport in that specific laser material.

REFERENCES

[1] M. Razeghi, "Optoelectronic Devices Based on III-V Compound Semiconductors Which Have Made a Major Scientific and Technological Impact in the Past 20 Years," IEEE J. on Selected Topics in Quant Elect., **6**(6), pp. 1344-1354 (2000).

[2] J. J. Coleman, "Strained-Layer InGaAs Quantum-Well Heterostructure Lasers," IEEE J. on Selected Topics in Quant. Elect., **6**(6), pp. 1008-1013 (2000).

[3] B. D. Evans, H. E. Hager and B. W. Hughlock, "5.5 MeV Proton Irradiation of a Strained Quantum Well Laser Diode and a Multiple Quantum-Well Broadband LED," IEEE Trans. Nucl. Sci. **40**(6), pp. 1645-1654 (1993).

[4] Y. F. Zhao, *et al.*, "200 MeV Proton Damage Effects on Multi-Quantum Well Laser Diodes," IEEE Trans. Nucl. Sci., **44**(6), pp. 1898-1905 (1997).

[5] A. H. Johnston, T. F. Miyahira and B. G. Rax, "Proton Damage in Advanced Laser Diodes," IEEE Trans. Nucl. Sci., **48**(6), pp. 1764-1772 (2001).

[6] H. Schöne, *et al.*, "AlGaAs Vertical-Cavity Surface-Emitting Laser Responses to 4.5-MeV Proton Irradiation," IEEE Phot. Tech. Lett., **9**(12), pp. 1552-1554, 1997.

[7] A. Kalavagunta, *et al.*, "Effects of 2-MeV Proton Irradiation on Operating Wavelength and Leakage Current of Vertical Cavity Surface Emitting Lasers," IEEE Trans. Nucl. Sci., **50**(6), pp. 1982-1990 (2003).

[8] B. Witxigmann and M. S. Hybertsen, "A Theoretical Investigation of the Characteristic Temperature T_0 for Semiconductor Lasers," IEEE J. of Selected Topics in Quantum Electronics, **9**(3), pp. 807-815 (2003).

[9] B. H. Rose and C. E. Barnes, ""Proton Damage Effects on Light-Emitting Diodes," J. Appl. Phys., **53**(3), pp. 1772-1780 (1992).

[10] P. W. A. McIlroy, A. Kurobe and Y. Uematsu, "Analysis and Application of Theoretical Gain Curves to the Design of Multi-Quantum-Well Lasers," IEEE J. Quant. Elect., **21**(12), pp.1958-1963 (1985).

[11] L. A. Coldren and S. W. Corzine, *Diode Lasers and Photonic Integrated Circuits*, John Wiley: New York, 1995.

[12] J. Minch, *et al.*, "Theory and Experiment of InGaAsP in InGaAlAs Long-Wavelength Strained Quantum-Well Lasers," IEEE J. Quant. Electron., **35**(5), pp. 771-782 (1999).

[13] P. L. Derry, *et al.,* "Low Threshold Current High-Temperature Operation of InGaAs/AlGaAs Laser Diodes," IEEE Photon. Technol. Lett., **4**(11), pp. 1189-1191 (1992).

[14] A. B. Campbell, *et al.*, "Particle Damage Effects in GaAs JFET Test Structures," IEEE Trans. Nucl. Sci., **33**(6), pp. 1435-1441 (1986).

[15] J. G. Williams, *et al.*, "Carrier Removal and Changes in Electrical Properties of Neutron Irradiated GaAs," J. Appl. Phys., **70**(9), pp. 4931-4937 (1991).

[16] J. L. Pankove, "Temperature Dependence of Emission Efficiency and Lasing Threshold in Laser Diodes," IEEE J. Quantum Electron., **4**, pp. 119-122 (1968).

[17] D. A. Ackerman, et al., "Analysis of Gain in Determining To in 1.3 μm Semiconductor Lasers," IEEE J. of Select. Topics in Quantum Electron., **1**(2), pp.250-263 (1995).

[18] Y. Zou, *et al.*, "Experimental Study of Auger Recombination, Gain, and Temperature Sensitivity of 1.5 μm Compressively Strained Semiconductor Laser," IEEE J. Quantum Electron., **29**(6), pp. 1565-1575 (1993).

End of File